The Influence of Oxygen-Enriched Burner Systems on the Scale Formation of Steel Alloys During Heating Processes

Dipl.-Ing. Christina Sobotka[1], Prof. Helmut Antrekowitsch[1], Dr. Holger Schnideritsch[1]

[1]Institute of Nonferrous Metallurgy, Montanuniversitaet Leoben
Franz-Josef-Straße 18,
8700 Leoben, Austria
Phone: 0043 3842 402 5200
Email: Christina.sobotka@unileoben.ac.at

Keywords: oxidation, high temperature corrosion, oxygen enrichment, oxygen enhanced burners, 42CrMo4, H525, scale formation

ABSTRACT

The influence of oxygen enrichment on the scale formation of steel alloys in burner fired furnaces is investigated. Oxygen enriched combustion leads to a higher amount of oxidising agents (CO_2 and H_2O) in the atmosphere which react with the steel surface during the heating process and affects the high-temperature oxidation. Therefor experiments with four steel grades are carried out using thermogravimetric analyses and various oxygen enrichment grades (23 % O_2 enhanced, 30 % O_2 enhanced combustion and 100 % oxyfuel combustion) are compared with oxidation in air fired atmosphere. The results imply that there is a change in the kinetic model of the oxidation reaction at a temperature above 1000 °C. The morphology of the oxide layers were analyzed using scanning electron microscopy (SEM) in combination with energy dispersive x-ray spectroscopy

INRODUCTION

In the metallurgy ways to improve efficiency and cut operation costs with low investments are always sought for. Forging, reheating and heat treatment furnaces are usually heated with natural gas burners. The combustion efficiency can be increased using oxygen enhanced combustion. Higher concentrations of oxygen in the combustion process reduce the amount of nitrogen ballast and increase the thermal efficiency. Less nitrogen results in a lower amount of exhaust gas volume and leads to a higher concentration of highly radiating products as CO_2 and H_2O. With lower nitrogen concentration the NO_x emissions are beneficially reduced as well. Oxygen enhancement can reduce fuel consumption as well as save energy up to 50 %. Another positive effect is that the combustion emissions are reduced and the steel production can be increased due to the faster heating rates and equally higher furnace throughput. In this paper the impact of oxygen enhanced combustion on the oxidation behaviour of four steel grades is studies in comparison with conventional air fired burner systems.

OXIDATION PRINCIPLES

The reaction of metal with oxygen is dependent on the thermodynamics and kinetics of the oxidation. The thermodynamics indicates whether a reaction is energetically possible. The thermodynamics describes the stability of phases in equilibrium at ambient conditions. The formation of iron oxides proceeds at lowest pressures, so the oxidation cannot totally be avoided. The formation of scale at elevated temperatures under an oxidizing atmosphere can be described in three steps: [1; 2]

1. Reaction at the outer interface metal oxide/gas: oxygen transfer through the gas phase in the metal oxide phase

2. Diffusion of the oxygen or the metal through the oxide layer

3. Chemical reaction at the inner phase surface metal oxide/metal: transfer of the metal from the substrate into the oxide

The reaction rate is determined by the kinetics. Depending on the temperature range the oxidation may follow different mathematical approaches. At temperatures below 300 °C there is an initial rapid reaction, which decays with the time. These layers of approximately 100 nm follow a logarithmic oxidation rate. At a temperature between 300 to 450 °C the cubic oxide growth is valid. However in the metallurgy processes only high temperature relationships are applicable and certain two laws are applicable: the linear growth and the parabolic scaling rate. In Figure 1 the classification of high temperature oxidation kinetics is displayed. [3; 4; 2]

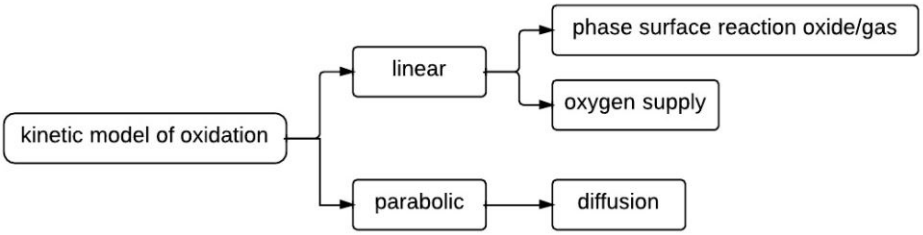

Figure 1. Classification of the limiting steps in high temperature oxidation kinetics

A linear oxidation rate occurs if either the gas surface reaction between the metal oxide and the gas atmosphere is rate limiting, or the oxygen supply at the surface is slower than the oxide formation. Which of the two high temperature laws is applicable determines whether the oxygen partial pressure in the atmosphere or the diffusion rate of the ions is the most effecting factor for the oxidation. If the reaction follows a linear oxide growth a higher oxygen concentration in the gas atmosphere reflects in increasing oxidation. And therefor an oxygen concentration gradient is formed. [3; 4; 2; 5]

In Figure 2 the reaction following the linear oxidation rate is exemplified. The concentration of oxidizing components of the surrounding atmosphere decreases nearby the metal oxide. The migration of the oxygen through the interface is the crucial factor for the oxidation reaction and gas flow rate has an impact on the oxidation reaction. Higher flow rates reduce the concentration gradient and result in a higher concentration of oxidizing components at the metal oxide surface.

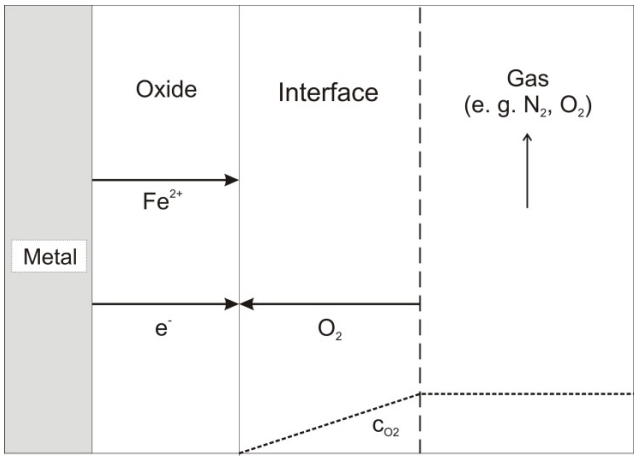

Figure 2. Linear law of kinetics

Literature says the linear oxidation rate is valid at thin oxide layers, but prior experiments [2] showed that high temperature above 900 °C leads to linear behavior too as a ion diffusion equilibrium is reached. At constant gas flow rate the scaling process follows a linear function.

$$\frac{ds}{dt} = konst. \tag{1}$$

$$s = konst. \cdot t \tag{2}$$

The oxide layer thickness is noted as s. Integrated and mass gain Δm per area A instead of the oxide layer thickness the linear oxide growth is formed:

$$k_l \cdot t = \frac{\Delta m}{A} \tag{3}$$

In equation (3) k_l is the linear oxidation constant. The linear oxidation rate is used for a restricted phase surface reaction and low concentration of oxidizing components or high oxidation rate, where the gas supply onto the surface is limiting. [6; 4]

If the parabolic oxidation rate is valid, the diffusion of the ions is the limiting step of the oxidation reaction. The mixture of the gas atmosphere has an inferior position. A schematic scale formation following the parabolic oxidation is displayed in Figure 3. In three cases the parabolic oxide growth occurs [7]:

a) The oxygen ion diffusion through the oxide layer is faster than the metal cations. The oxidation takes place at the inner surface metal/oxide (e. g. Fe_2O_3, SiO_2, TiO_2, ZrO_2, UO_2 and mostly Al_2O_3).

b) The metal cations diffuse faster than the oxygen anions. The oxide layer grows at the outer surface oxide/gas (e. g. CoO, Cr_2O_3, Cu_2O, FeO und NiO).

c) Both metal cations and oxygen anions diffuse faster than the electrons. The layer grows from inside to outside, depending which ions diffuse faster (e. g. Al_2O_3).

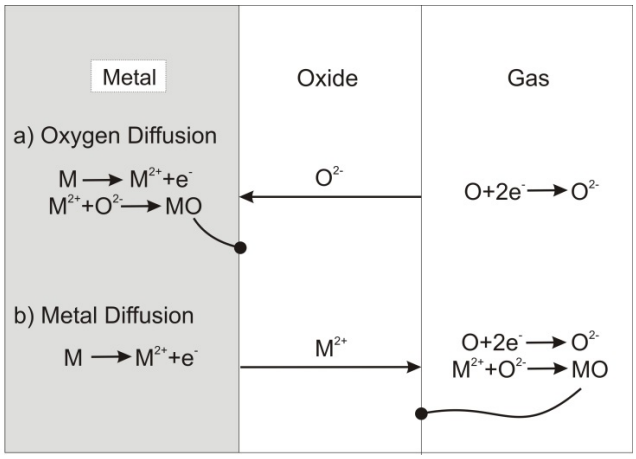

Figure 3. Parabolic law of kinetics

The parabolic reaction equation was first derivated by Tammann in 1920 and is used in several publications [8; 9; 3; 10–12]:

$$\frac{ds}{dt} = \frac{k}{s} \tag{4}$$

The oxide layer thickness is noted as s. Integrated with $\Delta s = 0$ für $t = 0$ and mass gain Δm per area A instead of the oxide layer thickness the parabolic oxide growth is formed (see equation (5)). k_p is the parabolic oxidation constant. If the parabolic oxidation rate is valid, the mass gain Δm over the time t has to display a parable.

$$\left(\frac{\Delta m}{A}\right)^2 = k_p t \tag{5}$$

EXPERIMENTAL PROCEDURES

The experiments in this study investigate the influence of oxygen enrichment on the scaling principles. The oxidation took place under the combustion atmosphere of air, 23 %, 30 % oxygen enhanced and 100 % oxyfuel combustion. The oxygen enrichment states depict the typical industrial enhancements. Up to 30 % O_2 an existing air burner can modified to use it as an O_2 enhanced combustion burner. For higher level enrichment a special oxyfuel burner is used. The higher the enrichment state the more beneficial effected is the combustion.

Four special alloys were analyzed using thermogravimetric analyses: low alloy mild steel, Cr-Mo steel (42CrMo4, 1.7225), Cr-Ni-Mn steel (H525, 1.4841, X15CrNiSi2521) and Fe-Cr-Al steel (Kanthal). The compositions of the four steel grades are noted in Table 1.

Table 1. Nominal composition using XRF and X-ray spectroscopy of alloys tested

Steel alloy	Fe [%]	C [%]	Si [%]	Mn [%]	P [%]	S [%]	Cr [%]	Ni [%]	Mo [%]	Al [%]	Cu [%]	Co [%]	N [%]	Zr [%]	As [%]	Sn [%]	V [%]
Mild steel	97.94	0.23	0.183	0.69	0.026	0.026	0.14	0.157	0.018	<0.001	0.187	0.011	0.014	-	0.011	0.037	-
Cr-Mo steel	97.41	0.40	0.249	0.66	0.013	0.013	0.97	0.029	0.180	0.022	0.024	0.0036	0.008	-	0.007	0.007	-
Cr-Ni-Mn	53.20	0.03	2.26	1.64	0.022	0.002	23.07	19.01	0.226	0.018	0.184	0.075	0.027	-	0.024	0.015	0.108
Fe-Cr-Al	70.15	0.05	0.211	0.08	0.012	0.007	23.48	0.270	0.016	5.47	0.0085	0.07	0.035	0.178	-	-	0.04

In Table 2 the oxidizing gas mixtures are listed. The content of the atmospheres depends on the combustion process. O_2 enhanced combustion leads to less N_2 in the air. With increasing O_2-enrichment the H_2O and CO_2 content in the furnace rises. Especially water vapour and CO_2 act as oxidizing agents and influence the scale formation.

Table 2. Oxidation atmosphere correlating with Industrial furnace atmosphere in dependence of the combustion parameters

O_2-enhanced combustion	CO_2 [vol.-%]	N_2 [vol.-%]	O_2 [vol.-%]	H_2O [vol.-%]
21 % O_2 (= air)	8.7	72.2	2.1	17.1
23 % O_2	9.6	69.7	1.9	18.8
30 % O_2	12.3	61.5	2.0	24.3
100 % O_2	33.2	0.0	1.3	65.5

The thermogravimetric analyses were performed in a way to perfectly depict the process of burner fired reheating, heat treatment or forging furnaces. Continuous isothermal oxidation tests were carried using a NETZSCH STA 449 F3 with a water vapour furnace and a water vapour generator in TG mode with high-resolution (1 µg) microbalance. The schematic procedure of the experiments is shown in Figure 5.

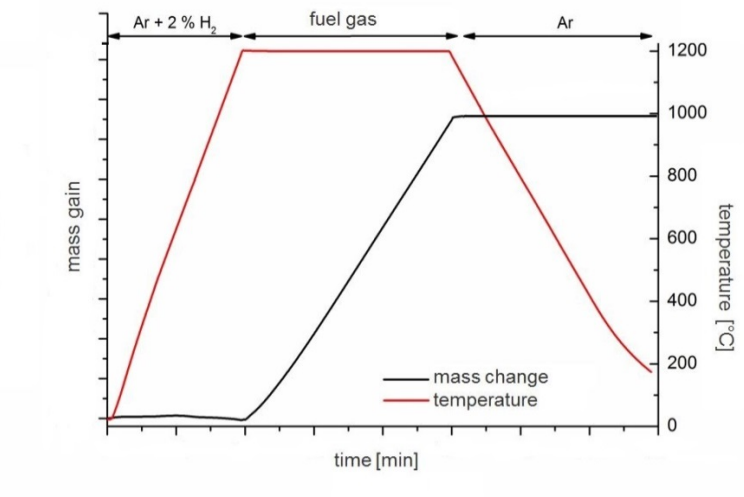

Figure 4. Schematic procedure of the heating rate, used gases and mass gain of the experiments

The steel alloys are investigated under different atmospheres correlating to industrial heating and forging furnaces to show the influence of oxygen enhanced combustion in a temperature range from 750 °C to 1200 °C. The test procedure consisted of heating the sample under gas Ar + 2 % H_2 to the target temperature with a heating rate of 10 K/min. The marginal hydrogen concentration prevents the specimen of oxidizing before reaching the isothermal temperature. This is very important for the kinetic analyses of the oxidation [13]. The specimen was held under the combustion atmosphere for three hours and continuously monitored by weight change. Then it was cooled down under Argon to room temperature to preserve the oxide. Cylindrical specimens with dimensions 14 mm in diameter by 2 mm in height were cut out of the master alloy so that each specimen fitted onto the Al_2O_3 crucible and grinded with P220 sand paper. The Al_2O_3 crucible was prior spray coated with BN to prevent to reaction of the steel with the Al_2O_3 plate. The total surface area for each specimen was measured to relate the mass change to its initial area. A blank baseline was first obtained with the empty crucible at the temperature profile and gas flow rate of interest. Then the experiment with specimen on the crucible under the same conditions was carried out. The baseline is used to correct the effect of the gas flow on the high sensitivity microbalance system.

Two steel grades, Cr-Mo steel (42CrMo4) and mild steel were examined over the full oxygen enrichment levels (21 %, 23 %, 30 % and 100 %), stack oxygen concentration approximately 2 % at temperatures of 750 °C, 850 °C, 950 °C, 1050 °C, 1150 °C and 1200 °C over a duration time of 180 minutes. Two additional steel grades, Cr-Ni-Mn steel (H525) and Fe-Cr-Al steel (Kanthal), were tested under the same parameter, but at temperatures of 950 °C, 1050 °C, 1150 °C and 1200 °C, as pretests showed that lower temperatures do not effect these high temperature alloys [14].

RESULTS AND CHARACTERISATION

The results of the thermodynamic analyses display the mass gain of the specimen during three hours oxidation under flue gas from air combustion up to 100 % oxygen enrichment. The test results were examined regarding the kinetic behavior of the oxidation with respect to the four oxygen enriched combustion states (21 %, 23 %, 30 % and 100 % O_2). The scaling rate data generally follow either the parabolic oxidation or the linear oxidation. The two forms of kinetic oxidation rates distinguish whether the concentrations of oxidizing elements in the gas phase or the diffusion rate of the ions effect the reaction primarily. The data were fitted to the models in form of:

Linear oxidation rate: $\frac{\Delta m}{A} = k_l \cdot t \rightarrow y = k_l \cdot t$ (6)

Parabolic oxidation rate: $\left(\frac{\Delta m}{A}\right)^2 = k_p t \rightarrow y^2 = k_p \cdot t$ (7)

The intercept is zero as the oxidation starts right away if the oxidizing atmosphere is passed into the thermogravimetric furnace. Through comparison of the R^2 the model characterizing the oxidation at certain parameters (alloy, temperature and gas) is validated. For the graphic analyses the software OriginPro 9.0 was used. The quality of a regression model can be

measured with the coefficient of determination R^2. The R^2 indicates the % of variability of the dependent variable which is explained by the explanatory variables and is calculated following equation (8) to (12). In equations (9) and (10) TSS is the sum of squares, RSS is the residual sum of squares. For full fitted behavior, we would expect a R2 = 1 in these relationships. The corrected coefficient of determination $\bar{R}^2$ is calculated with the degree of freedom and is the best measurement for the validation of the regression model.

$$w_i = \frac{1}{\sigma_i^2} \tag{8}$$

$$TSS = \sum_{i=1}^{n} w_i (y_i - \bar{y})^2 \tag{9}$$

$$RSS = \sum_{i=1}^{n} w_i (y_i - \hat{y}_i)^2 \tag{10}$$

$$R^2 = 1 - \frac{RSS}{TSS} \tag{11}$$

$$\bar{R}^2 = 1 - \frac{\frac{RSS}{df_{Error}}}{\frac{TSS}{df_{Error}}} \tag{12}$$

Cr-Mo steel

The isothermal oxidation tests of the steel alloy 42CrMo4 were performed from 750 °C to 1200 °C at 3 hours exposure time in 21 % air combustion atmosphere, 23 % and 30 % oxygen enhanced combustion atmosphere as well as in 100 % oxyfuel combustion flue gas. The scaling rate data was investigated concerning its kinetic mechanism. The parameters of the oxidation rate following equation (6) and (7) are listed in Table 3. The oxidation rate rises with increasing temperature and higher concentration of oxidizing components of the atmosphere. The rate constant is highest for oxidation under 100 % oxyfuel combustion gas and a temperature of 1200 °C. Comparing the corrected coefficient of determination $\bar{R}^2$ in Table 3 a change from parabolic to linear behavior takes place at a temperature of 1050 °C under air, 23 % and 30 % oxygen enriched combusted off gas. Under full oxyfuel combustion flue gas the 42CrMo4 show full parabolic scaling rates at all temperatures.

Table 3: Parameters of the oxidation rate through the mass gain of the alloy 42CrMo4 after three hours tests

		Parabolic oxidation rate ←						→ Linear oxidation rate						
Gas combustion	Fit	750 °C		850 °C		950 °C		1050 °C		1150 °C		1200 °C		
		k	$\bar{R}^2$	k	$\bar{R}^2$	k	$\bar{R}^2$	k	$\bar{R}^2$	k	$\bar{R}^2$	k	$\bar{R}^2$	
Air	Linear	0,001	0,973	0,002	0,982	0,003	0,965	**0,005**	**0,995**	**0,013**	**0,997**	**0,017**	**0,997**	
	Parabolic	**1,55E-4**	**0,997**	**4,49E-4**	**0,993**	**0,001**	**0,9980**	0,004	0,959	0,023	0,964	0,038	0,967	
23 % enhanced	Linear	0,00111	0,979	0,00209	0,988	0,00362	0,976	**0,00719**	**0,995**	**0,014**	**0,996**	**0,016**	**0,998**	
	Parabolic	**1,58E-4**	**0,990**	**5,61E-4**	**0,988**	**0,00166**	**0,994**	0,00676	0,971	0,027	0,968	0,034	0,957	
30 % enhanced	Linear	0,00112	0,979	0,00221	0,982	0,0037	0,977	**0,0066**	**0,996**	**0,0141**	**0,993**	**0,017**	**0,992**	↑ gas controlled
	Parabolic	**1,63E-4**	**0,988**	**5,61E-4**	**0,992**	**0,00174**	**0,994**	0,00574	0,964	0,026	0,977	0,037	0,982	
100 % oxyfuel	Linear	0,0012	0,972	0,003	0,978	0,005	0,982	0,009	0,974	0,017	0,971	0,020	0,974	↓ diffusion controlled
	Parabolic	**1,81E-4**	**0,998**	**0,001**	**0,995**	**0,003**	**0,992**	**0,009**	**0,977**	**0,038**	**0,994**	**0,053**	**0,997**	

As Table 3 depicts under a temperature of 1050 °C the oxidation follows the parabolic rate law. The diffusion is the limiting step of the oxide growth. The diffusion coefficient in solids is temperature dependent and with rising temperature the diffusion of the ions increases. This correlates with a change of oxidation kinetics above 1050 °C to linear oxidation rate. From 1050 °C to 1200 °C the supply of the oxidizing components in the gas atmosphere becomes determining. This phenomenon is observed from air combustion atmosphere up to 30 % oxygen enhanced combustion gas. 100 % oxyfuel combustion atmosphere shows a different behavior. As there are much more oxidizing compounds available (33,2 % CO_2, 65,5 % N_2 and 1,3 % O_2) the gas supply and phase surface reaction become less determining. There is enough oxidator at the

phase surface available and the limiting factor is the diffusion of the ions through the oxide layer. In Figure 5 the test results of three hours oxidation under air combusted flue gas are displayed. The mass gain was continuously monitored by the high resolution balance system. In Figure 6 the linear oxidation rate is plotted versus the time and in Figure 7 the parabolic oxidation rate is noted. For temperatures above 1050 °C the linear regression model fits better as the interrupted line, which corresponds to the fit, shows. This results in a higher $\overline{R}^2$. As you can see the interrupted line in Figure 7 has a greater deviation and no parabolic behavior is valid.

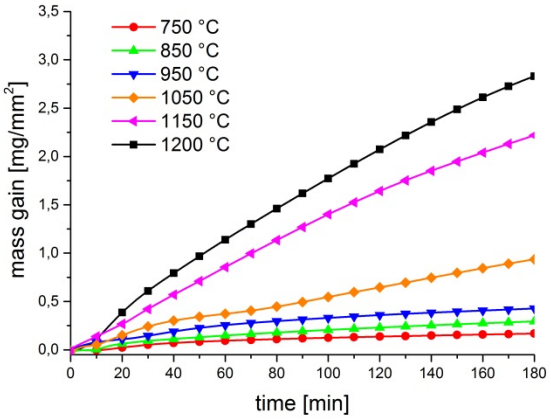

Figure 5. Oxidation rate of the alloy 42CrMo4 under air combusted flue gas

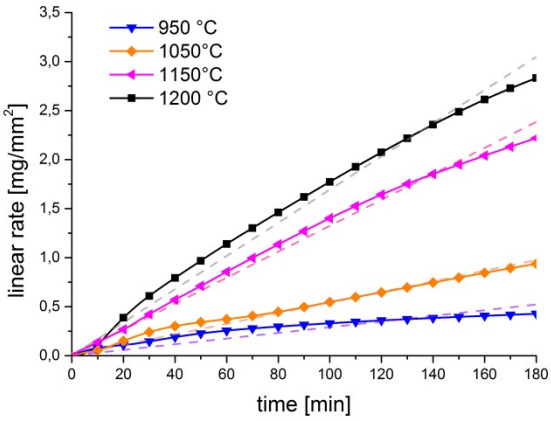

Figure 6. Linear fitted oxidation rate 42CrMo4 under air combusted flue gas

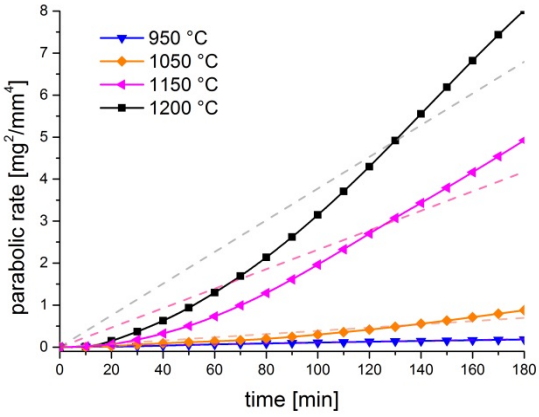

Figure 7. Parabolic fitted oxidation rate 42CrMo4 under air combusted flue gas

The contrary phenomenon can be observed for the experiments under 100 % oxyfuel combusted gas. Figure 8 left shows the mass gain throughout the oxidation test. There is an increase in oxidation above 1050 °C. The parabolic oxidation rate fits perfectly at all temperatures. The oxide formation shows full parabolic behavior, even at high temperatures.

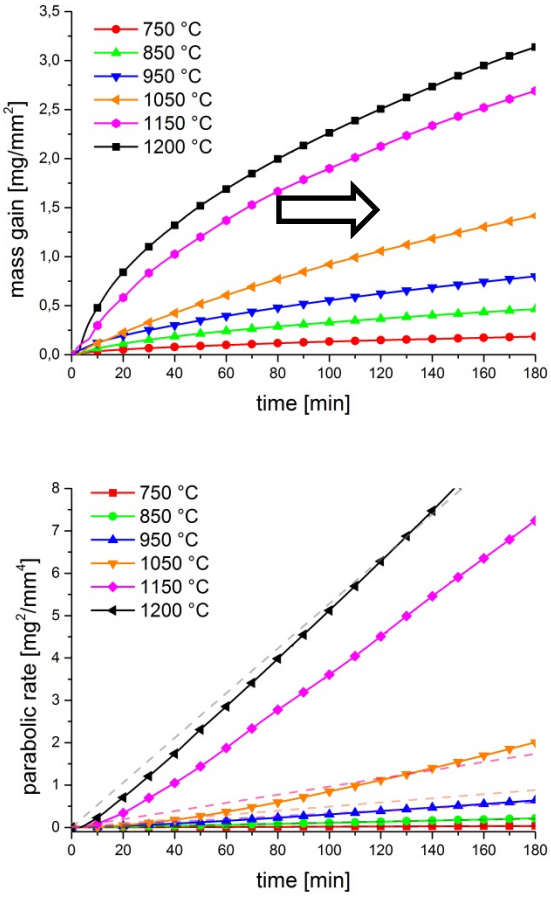

Figure 8. Oxidation rate 42CrMo4 under 100 % oxyfuel combustion (left) and parabolic rate constant incl. fitted graph

Figure 9 gives a graphic overview of the rate constants of the oxidation from 750-1200 °C. Up to 30 % oxygen enrichment leads to no distinct increase of oxidation, at a temperature of 1200 °C the parabolic constant varies between 0,016-0,017 mg2/mm4. Above a temperature of 1150 °C oxyfuel combustion causes more scale formation, in comparison to the results of lower oxygen enrichment stated oxyfuel combustion leads to a parabolic rate constant of 0,053 mg2/mm4. The oxidation data is displayed in Table 3.

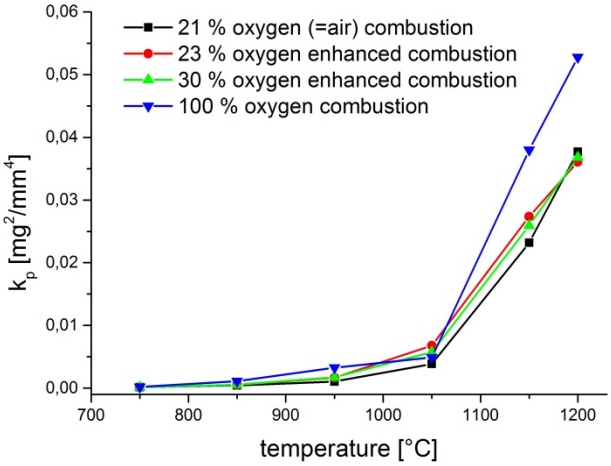

Figure 9. Influence of the combustion atmosphere on the rate constant for the oxidation from 750-1200 °C of the alloy 42CrMo4

The morphology of the oxide layer of the high temperature resistant steel alloys was analyzed using scanning electron microscopy (SEM) in combination with energy dispersive x-ray spectroscopy. The oxide scale formed in alloy 42CrMo4 at 1150 °C from oxidation in 23 % oxygen enhanced combustion atmosphere is shown in Figure 10. The EDS analysis indicates that the oxide scale is predominantly iron oxide with manganese. The concentration of chromia is decreasing with oxide thickness. On the right side of Figure 10 interface metal substrate/oxide is magnified. There is a loose attachment with loads of pores resulting of the oxidation of the carbon content of the steel and formation of CO_2 inside the layer.

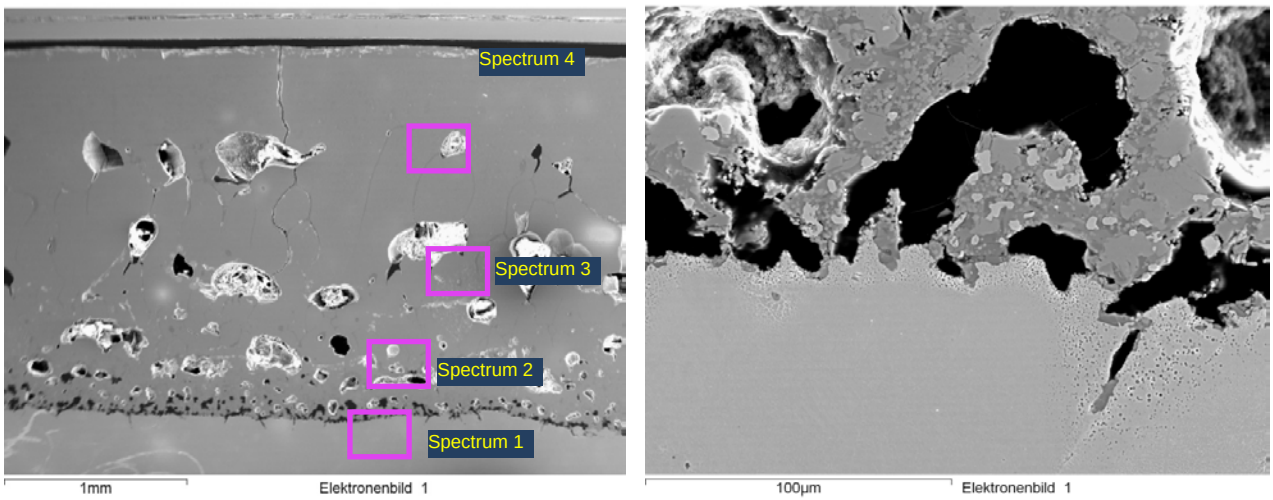

Figure 10. Scale morphology of the Fe-Cr steel after three hours at 1150 °C in 23 % oxygen enhanced combusted atmosphere, left: with concentration gradient, right: metal/oxide interface

Table 4. Chemical composition according to EDS-analyses of the oxide layer Fe-Cr steel after three hours at 1150 °C in 23 % oxygen enhanced combusted atmosphere

Spectrum	O	Si	Cr	Mn	Fe	Mo
1		0.41	1.00	0.74	97.85	
2	15.18	1.44	4.41	0.58	77.66	0.74
3	14.22	0.49	0.66	0.53	84.10	0.00
4	14.79			0.78	84.43	

Consistent with the thermogravimetric results, Figure 11 illustrates that corrosion of the alloy 42CrMo4 under 100 % oxyfuel combustion atmosphere is more severe. In both cases at 1150 °C, the scale appears porous but still attached to the metal substrate. EDX-analyses show that Cr-oxide is found in the oxide directly attached to the substrate. With oxide growth the Cr-concentration decreases resulting in a Cr-gradient towards the gas phase. At the interface oxide/substrate segregation takes place as there are found oxide grains with silicon and phosphor (spectrum 7) and ones with molybdenum (spectrum 6) as there is a silicon gradient and a molybdenum gradient towards the metal substrate. In the outer oxide these two elements are according to EDX-analyses no longer part of the oxide layer. The SEM micrograph in Figure 11 shows that in this 42CrMo4 alloy, with oxidation in 100 % oxyfuel combustion atmosphere at 1150 °C, there is an outward growth of oxide grains that have sintered together.

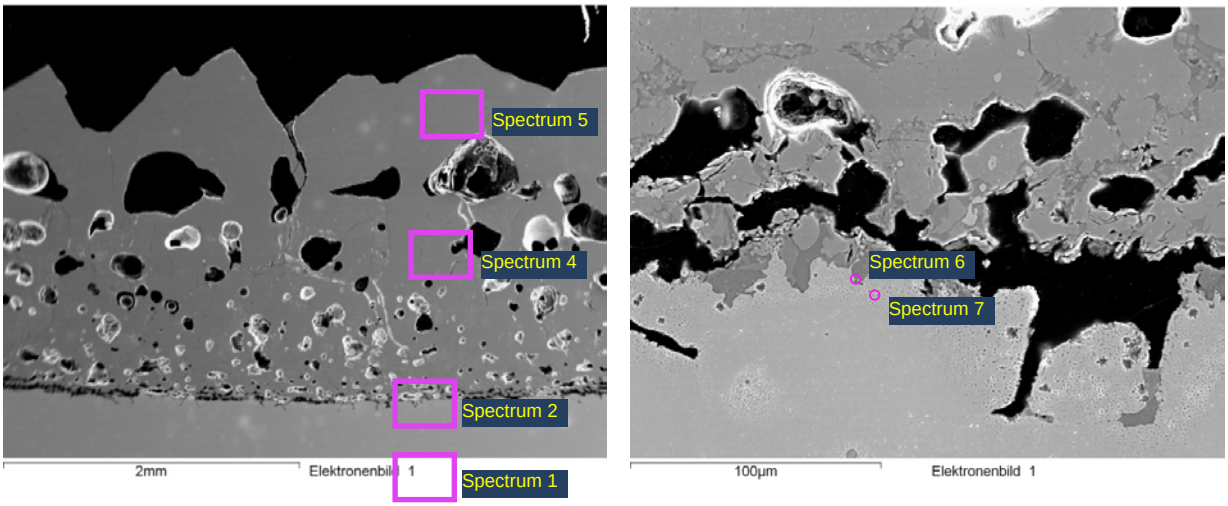

Figure 11. Scale morphology of the Fe-Cr steel after three hours at 1150 °C in 100 % oxyfuel combustion atmosphere

Table 5. Chemical composition according to EDS-analyses of the oxide layer Fe-Cr steel after three hours at 1150 °C in 100 % oxyfuel combustion atmosphere

Spectrum	O	Si	Cr	Mn	Fe	Mo
1			1.07	0.85	97.58	0.50
2	14.13	0.99	4.10	0.57	79.31	0.90
4	14.07			0.68	85.26	
5	14.19			0.67	85.14	14.19
6	16.62		1.49	0.57	80.48	0.85
7	19.49	15.65	0.37	1.28	63.21	

Low alloy mild steel

The thermogravimetric results of the low alloy mild steel were evaluated like the results of the 42CrMo4 and the system of kinetic analyses remained the same. At a temperature of 1050 °C the parabolic oxidation rate changes into linear oxidation for reaction under gas up to an oxygen enrichment of 30 %. In Table 6 is noted that oxidation under full oxygen combusted atmosphere shows full parabolic behavior and is not phase surface controlled. The oxidizing components supply (e. g. O_2, CO_2 and H_2O) onto the reaction surface is fast enough that the diffusion of the reacting agents becomes rate limiting.

Table 6. Parameters of the oxidation rate through the mass gain of the mild steel after three hours tests

		Parabolic oxidation rate ←						→ Linear oxidation rate						
Gas combustion	Fit	750 °C		850 °C		950 °C		1050 °C		1150 °C		1200 °C		
		k	$\bar{R}^2$	k	$\bar{R}^2$	k	$\bar{R}^2$	k	$\bar{R}^2$	k	$\bar{R}^2$	k	$\bar{R}^2$	
Air	Linear	0,001	0,975	0,002	0,951	0,003	0,974	**0,008**	**0,997**	**0,011**	**0,996**	**0,012**	**0,998**	
	Parabolic	**1,862E-4**	**0,997**	**3,024E-4**	**0,999**	**0,002**	**0,994**	0,007	0,966	0,017	0,971	0,020	0,918	
23 % enhanced	Linear	0,00113	0,979	0,00219	0,969	0,005	0,97314	**0,009**	**0,989**	**0,009**	**0,997**	**0,010**	**0,996**	
	Parabolic	**1,617E-4**	**0,995**	**6,052E-4**	**0,999**	**0,003**	**0,99799**	0,010	0,987	0,015	0,953	0,018	0,914	
30 % enhanced	Linear	0,00116	0,981	0,00172	0,953	0,005	0,97073	**0,008**	**0,998**	**0,012**	**0,999**	**0,014**	**0,994**	
	Parabolic	**1,712E-4**	**0,993**	**3,697E-4**	**0,999**	**0,003**	**0,99774**	0,008	0,931	0,019	0,947	0,024	0,977	↑ gas controlled
100 % oxyfuel	Linear	0,00144	0,973	0,0029	0,972	0,005	0,97352	0,008	0,985	0,016	0,984	0,021	0,966	
	Parabolic	**2,613E-4**	**0,997**	**0,001**	**0,998**	**0,003**	**0,99778**	**0,008**	**0,992**	**0,032**	**0,993**	**0,055**	**0,999**	↓ diffusion controlled

Figure 12 shows the parabolic rate constant versus the temperature for all tested gases. Similar to the results of the alloy 42CrMo4 the oxidation constant increases with the temperature. Air combustion, 23 % oxygen enhanced and 30 % oxygen enhanced combustion atmosphere show the same effects. Under pure oxyfuel combusted off gas the oxidation increases upon a temperature of 1050 °C showing its higher corrosiveness. At a temperature of 1200 °C the parabolic constant varies from air to 30 % oxygen enhanced combustion between 0,012-0,014 mg^2/mm^4. Above a temperature of 1150 °C oxyfuel combustion causes more scale formation, in comparison to the results of lower oxygen enrichment stated oxyfuel combustion leads to a parabolic rate constant of 0,055 mg^2/mm^4.

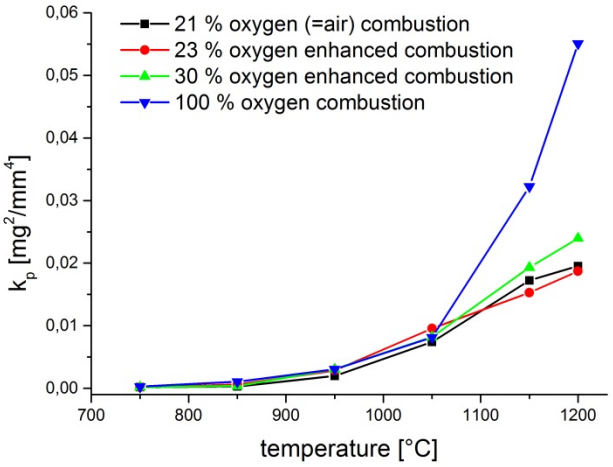

Figure 12: Influence of the combustion atmosphere on the rate constant for the oxidation from 750-1200 °C of the mild steel

The SEM-micrograph in Figure 13 shows that the mild alloy, with oxidation under 100 % oxyfuel combusted atmosphere at 1150 °C, forms two oxide layers. The inner layer consists of mainly iron oxide with chromia and manganic oxide, whereas in the outer oxide layer no chromia was found by EDX-analyses. In the inner oxide layer special Cu-oxide grains are found where arsenic and tin segregated inside. These alloying elements come from steel production out of secondary scrap metal and are very low in concentration in the metal substrate. Copper acts as a collector for impurities during the oxidation as the solubility of As and Sn in copper is very high. In Table 7 spectrum 1 is always the reference metal substrate. The concentration of silicon and copper decreases with growing oxide layer (see spectrum 3-5).

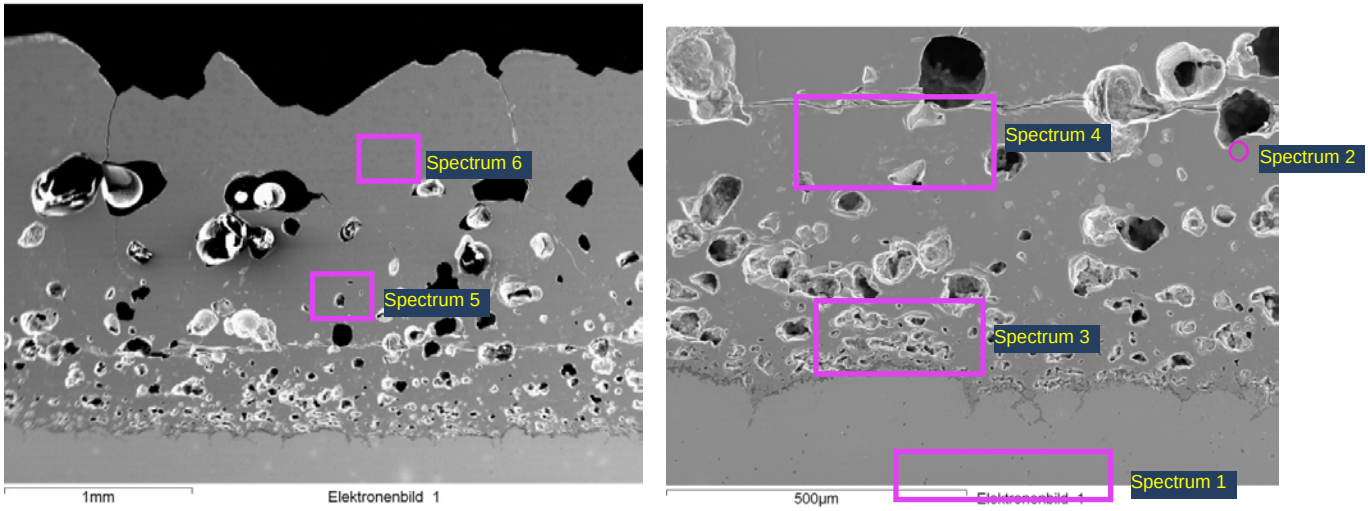

Figure 13. Scale morphology of the low alloy mild steel after three hours at 1150 °C in 100 % oxyfuel combustion atmosphere

Table 7. Chemical composition according to EDS-analyses of the oxide layer mild steel after three hours at 1150 °C in 100 % oxyfuel combustion atmosphere

Spectrum	O	Si	Cr	Mn	Fe	Ni	Cu	As	Sn
1		0.32	0,15	0.71	98.02		0.80		
2					4.70	6.42	82.96	1.57	4.34
3	13.25	1.31	0.36	0.62	82.97	0.44	1.04		
4	13.29	0.41	0.55	0.64	84.35		0.76		
5	13.66	0.26		0.57	85.51				
6	14.18			0.72	85.10				

In Figure 14 the magnification of the interface metal substrate/oxide is illustrated. Several oxide grains are grown inside the metal and a concentration mapping was performed (see left side of Figure 14). The oxide mainly consists of silicon with surrounding copper oxide and small amount of nickel oxide, which segregate along the grain boundary.

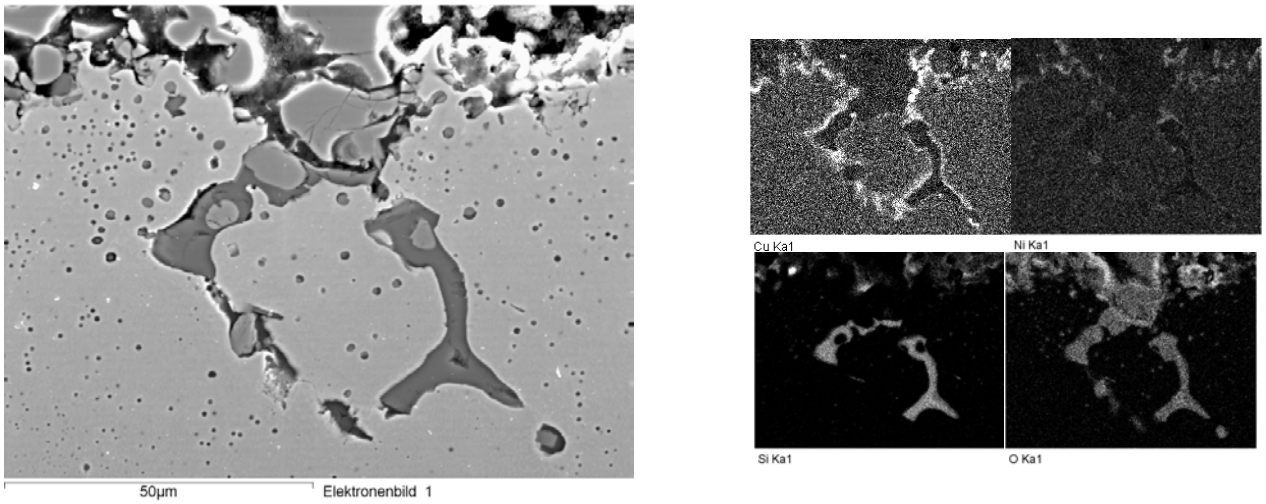

Figure 14. Magnification of the interface substrate/oxide of the low alloy mild steel after three hours at 1150 °C in 100 % oxyfuel enhanced combustion atmosphere

Cr-Ni-Mn steel

Ni alloyed steels are used up to 1000 °C for high-temperature and high-strength applications. For above temperatures alloys with higher amounts than 20 % Cr and Al, Si, Ti, Mo, Co and W have to be used. These offer improved oxidation resistance. According to the material data sheet of the alloy tested it is hear resistant up to 1000 °C with good mechanical properties. In this study the heat resistance was tested up to a temperature of 1200 °C in a highly oxidative atmosphere according to furnace flue gas. [11; 15; 16]

The alloy H525 forms a protective, adherent oxide layer which stops further reaction. Figure 15 shows the oxidation rate exemplary for 1200 °C. The rate of oxidation significantly decreases after the initial rapid oxidation and formation of the adherent oxide layer. Change in the slope indicated cracks in the oxide observed for oxidation under 30 % oxygen enhanced combustion atmosphere for 1200 °C. Spalling of the scale leads to an anew reaction of the substrate surface with the oxygen in the gap and the formation of oxides starts again. Therefor at the end of the experiments there is more metal oxidised which results in higher mass gain in the thermogravimetric analyses (see Figure 15).

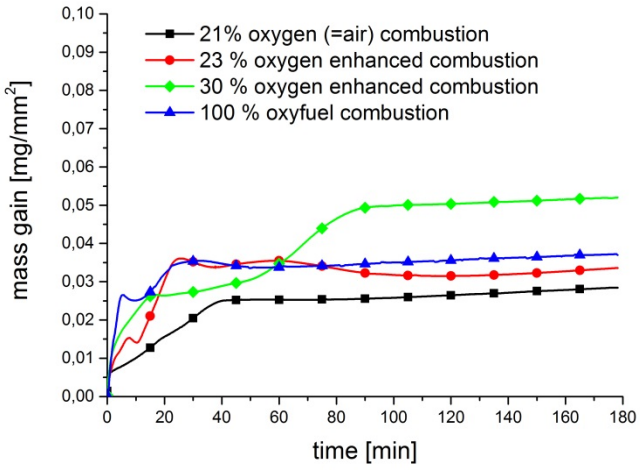

Figure 15. Oxidation rate of the alloy H525 at a temperature of 1200 °C for three hours

It is clear that experimental data deviate from the regression-fitted lines; however an approximate parabolic rate constant can be estimated. As Figure 15 shows the thermogravimetric analyses can be divided in two phases. First the initial oxidation and protective layer formation, second the steady-state mass gain as the protective layer stops further oxidation. In Table 8 oxidation kinetics are divided in two steps as well.

Table 8. Parameters of the oxidation rate at 1200 °C of the Cr-Ni-Mn steel after three hours tests

Gas combustion	Parabolic Fit	1200 °C	
		k_p	$\bar{R}^2$
Air	Initial oxidation (0-40 min)	1,41101E-5	0,98645
	Oxidation with protective layer	1,35578E-6	0,93511
23 % enhanced	Initial oxidation (0-40 min)	3,7598E-5	0,95325
	Oxidation with protective layer	1,31385E-6	0,35608
30 % enhanced	Initial oxidation (0-20 min)	4,61084E-5	0,99048
	Oxidation with protective layer (>min 90)	2,80292E-6	0,99406
100 % oxyfuel	Initial oxidation (0-40 min)	4,97075E-7	0,94545
	Oxidation with protective layer	1,92731E-6	0,95497

Figure 16 shows the scale morphology of the Cr-Ni-Mn steel after three hours at 1150 °C in 100 % oxyfuel combustion atmosphere. The concentration profile is noted in Table 9. Two adherent oxide layers are formed consisting mainly of iron-, chrome- and nickel oxide. A concentration gradient leads to higher amounts of Cr-, Mn- and Ni-oxide near the substrate. In the inner oxide phase fair Ni- and Cu-oxid grains can be found which results due to segregation of the Ni and Cu (see spectrum 3, Table 9). The scale is well attached to the body of the alloy, offering a more protective oxide scale that that formed on the Cr-Mo alloy 42CrMo4 and the mild steel.

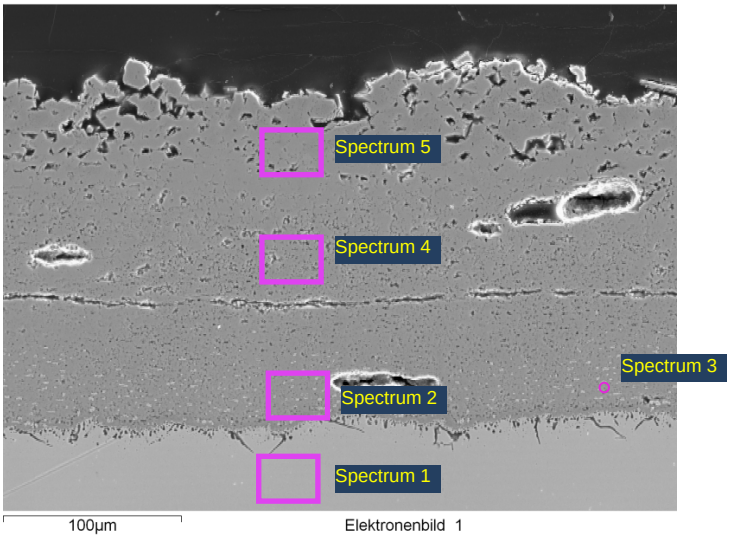

Figure 16. Scale morphology of the Cr-Ni-Mn steel after three hours at 1150 °C in 100 % oxyfuel combustion atmosphere

Table 9. Chemical composition according to EDS-analyses of the oxide Cr-Ni-Mo steel after three hours at 1150 °C in 23 % oxygen enhanced combusted atmosphere

Spectrum	O	Si	Cr	Mn	Fe	Ni	Cu
1		1.99	24.90	1.80	52.09	19.22	
2	14.78	1.41	33.42	1.11	28.83	20.45	
3	2.87		4.96		4.62	83.79	3,75
4	15.08	1.87	27.18	1.14	34.02	20.71	
5	15.19	0.34	13.42	1.59	56.30	13.16	

Fe-Cr-Al steel

Chromium, silicon and aluminum are the common alloying elements for high-temperature alloys due to the formation of protective Cr_2O_3, SiO_2 and Al_2O_3 oxide scales on the metal surface [17; 18]. The majority of commercially available high-temperature alloys form a chromia scale. For temperature resistance above 620 °C 12 % Cr steels or austenitic steel have to be used [11]. Figure 17 displayes the thermogravimetric analyses of the alloy Kanthal at a temperature of 1200 °C. The higher the amount of oxidizing compounds in the atmosphere the more oxide is formed, however the oxidation stops when a protective layer is formed. After the initial reaction of the substrate with the gas for some minutes (approx. 6 minutes) the oxidation rate decreases. In Figure 17 the oxidation under 100 % oxyfuel combustion starts at minute 20 again due to scale exfoliation and anew reaction of the metal substrate with the atmosphere. In Table 10 the parabolic rate constants for the oxidation at 1200 °C are noted. The constants are divided in the initial oxidation and further reaction if there is already an oxide layer formed.

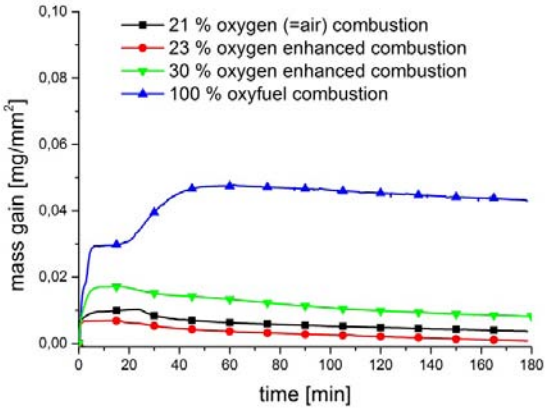

Figure 17. Oxidation rate of the alloy Kanthal at a temperature of 1200 °C for three hours

Table 10. Parameters of the oxidation rate at 1200 °C of the Fe-Cr-Al steel after three hours experiments

Gas combustion	Parabolic Fit	1200 °C	
		k_p	R^2
Air	Initial oxidation (0-2 min)	3,881E-5	0,913
	Oxidation with protective layer	2,235E-7	0,975
23 % enhanced	Initial oxidation (0-2 min)	2,755E-5	0,954
	Oxidation with protective layer	1,115E-7	0,950
30 % enhanced	Initial oxidation (0-6 min)	5,347E-7	0,994
	Oxidation with protective layer (>min 90)	9,488E-7	0,935
100 % oxyfuel	Initial oxidation (0-6 min)	1,869E-6	0,991
	Oxidation with protective layer	3,378E-6	0,986

Figure 18 illustrates the corrosion under 100 % oxyfuel combusted atmosphere at 1150 °C. The scale appears loosely attached to the body of the alloy. It is possible that the detachment of the scale from the body of the alloy was the result of sample molding and polishing in preparation for the SEM examination. The EDS analyses indicate that the oxide scale formed under combustion atmosphere is predominately iron oxide and chromia, Cr_2O_3 and containing some Al, Si. The highest concentration of aluminium and silicon oxide is found near the base material as the oxygen ion diffusion through the oxide layer is faster than the Al ion diffusion (see Spectrum 2 and 3). This phenomenon correlates with literature that says, that Al-oxides occur as subsurface scales mostly beneath the Cr-oxide that forms first [18]. The inner oxide layer appears strongly attached to the body of the alloy and looks less porous and more homogenous. If significant oxide spallation takes place, the inner oxide layer is continuous enough to stop further oxidation.

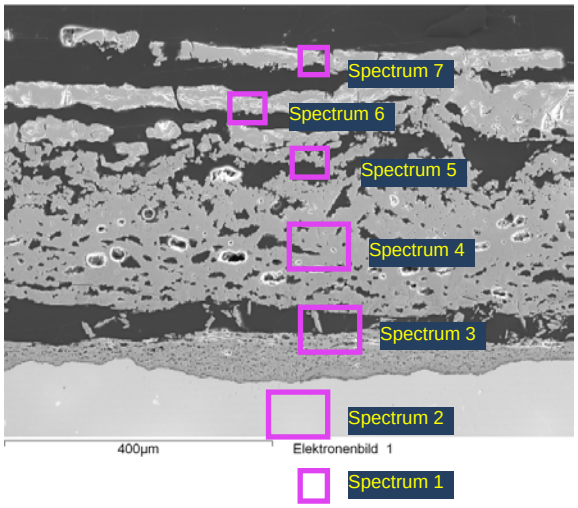

Figure 18. Scale morphology of the Fe-Cr-Al steel after three hours at 1150 °C in 100 % oxyfuel combusted atmosphere

Table 11. Chemical composition according to EDS-analyses of the oxide Fe-Cr-Al steel after three hours at 1150 °C in 100 % oxyfuel combusted atmosphere

Spectrum	O	Al	Si	Cr	Fe	Ni	Zr
1		3.87	0.33	21.33	74.05	0.42	
2	16.70	7.46	0.90	42.03	32.40	0.50	
3	17.12	9.36	0.50	38.29	34.73		
4	16.49	5.80	0.38	18.36	58.58		0.40
5	15.81	2.02	0.64	7.77	73.76		
6	14.97	0.35	0.66	0.44	83.59		
7	16.05	0.38	0.18	0.36	83.03		

DISCUSSION

The scale thickness increasing with temperature is apparent, particularly for oxidation in 100 % oxyfuel combusted atmosphere. Fe-Cr-Al steel and Cr-Ni-Mn steel resisted oxidation even in full oxygen enhanced combustion atmosphere at high temperatures better than the Cr-Mo steel and the mild steel. In case of the Cr-Mo steel and the mild, the growth of the oxidation product was significantly different depending on whether it originated by oxidation under 100 % oxyfuel combustion atmosphere or oxygen enhanced combustion. The scale of the alloy 42CrMo4 was much more porous. The oxide of the mild steel was firmly attached to the base alloy, an indication of fast diffusion of the metal ions from the body of the alloy to the reaction surface.

The thermogravimetric curves for the Fe-Cr-Al steel and Cr-Ni-Mn steel presented a shift in the oxidation rate after the initial oxidation that is an indication of early formation of a protective scale. The kinetic curves obtained by thermogravimetry of the Cr-Ni-Mn steel suggest that the scale formed early within the first 20-40 minutes of exposure to the flue gas, acting protectively and significantly reducing the rate of oxidation thereafter. A similar protective effect by the scale formed of the Fe-Cr-Al steel only takes place much sooner after approx. 2-6 min. The scale after oxidation by flue gas at all temperatures was sufficiently dense to act as a diffusion barrier over time as was evident by the plateau in the thermogravimetric curves (Figure 15 and Figure 17). The best corrosion protection is reached with a uniform, strongly adherent scale with no defect. The chance of exfoliation rises with mismatch of thermal expansion between alloy and scale and poor adhesion of the oxide layer to the matric.

This assessment indicates that oxidation resistance depends on factors such as alloy composition (metal diffusion rate to the surface), oxidizing atmosphere (CO_2, O_2 and H_2O content), and temperature. A significant factor, studied in previous work, is the relative surface roughness of the specimens that can affect nucleation for initial oxidation as well as the scale morphology.

CONCLUSION

In this work, an assessment was made by studying thermo-gravimetrically the oxidation rate of four steel alloys under air combusted atmosphere, 23 % and 30 % enhanced combustion atmosphere and 100 % oxyfuel combustion gas. While oxidation tests in forging, reheating and heat treatment furnaces can be complex, laboratory tests provide a good guidance for making preliminary selection how oxygen enrichment effects scale formation. The alloys tested were low alloy mild steel, Cr-Mo steel (42CrMo4, 1.7225), Cr-Ni-Mn steel (H525, 1.4841, X15CrNiSi2521) and Fe-Cr-Al steel (Kanthal) in the temperature range 750-1200 °C for 180 minutes duration time. The oxidation rate was measured by thermogravimetry and analyzed by means of the linear and parabolic rate law. If the linear rate law is valid the phase surface reaction and the supply of the oxidizing components of the gas atmosphere are rate limiting. The parabolic rate law is applicable, if the reaction is diffusion controlled, either by diffusion of the metal cautions through the oxide layer or by diffusion of the oxygen. In the case of the low alloy mild steel and the Cr-Mo steel under gas atmosphere from air up to 30 % oxygen enrichment at a temperature of 1050 °C the parabolic oxidation rate changes into linear oxidation. Under full oxygen combustion atmosphere the oxidation rate shows full parabolic behavior. Above a temperature of 1050 °C the oxidation rate increases using pure oxyfuel combustion atmosphere, whereas at lower temperatures oxygen enrichment does not effect the oxidation severely. The morphology of the oxide layers was analyzed using scanning electron microscopy (SEM) in combination with energy dispersive x-ray spectroscopy. The scales of the Cr-Mo steel and the mild steel have an overall porous appearance. However the oxide formed on the Cr-Mo steel is looser attached and there are a lot of pores at the interface metal substrate/oxide. Segregation of alloying elements took place at the inner oxide layer. In the oxide of the mild steel even small Cu-grains containing As and Sn were found. All four alloys showed a concentration gradient with decreasing content of chromia towards the outer oxide layer as the Cr-oxide layer forms first. The oxidation of the high temperature alloys Cr-Ni-Mn steel

and Fe-Cr-Al steel both formed a protective, adherent oxide layer, which stopped further oxidation. It mainly consisted of iron oxide and chromia and Ni-oxide in case of the Cr-Ni-Mn steel and Al-oxide in case of the Fe-Cr-Al alloy. The scale formed was sufficient dense to stop further diffusion and act as a barrier, corresponding with the plateau in the thermogravimetric analyses.

ACKNOWLEDGEMENTS

This work was initiated by Messer Group which established a technology competence center for metallurgy in 2005. The authors wish to thank Messer Group, the Austrian Research Promotion Agency (FFG) and the Austrian Federal Ministry of Economy, Family and Youth for supporting this project.

REFERENCES

1. S. Druecker: *Die Bildung und Vermeidung von Zunder beim Zweirollen-Gießverfahren*, TU Berlin, 2001.
2. C. Sobotka et al.: Investigation of the Scale Formation of a Chromium and Molybdenum containing Steel Alloy in an Oxipyr®-oxyfuel combusted Reheat Furnace. *Proceedings of European Metallurgical Conference EMC 2013 (*2013), pp 415–426.
3. C. Wagner: Der Angriff von Metallen durch Gase - 50 Jahre Grundlagenforschung: Rückblick und Ausblick. *Werkstoffe und Korrosion* 11 (1970), pp 886–893.
4. R. Viscorová: *Untersuchung des Wärmeübergangs bei der Spritzwasserkühlung unter Berücksichtigung des Einflusses der Verzunderung*, TU Clausthal, 2007.
5. A. Talekar et al.: Oxidation kinetics of high strength low alloy steels at elevated temperatures. *Corrosion Science 50* (2008), pp 2804–2815.
6. H. Selenz: *Ein Beitrag zum Verständnis der Verzunderung von Stahl in technischen Rauchgasen*, TU Berlin, 1980.
7. R. Bürgel et al.: Handbuch Hochtemperatur-Werkstofftechnik, *Springer Fachmedien Wiesbaden*, Wiesbaden, Auflage 4, 2011.
8. G. Tammann: Über Anlauffarben von Metallen. *Zeitschrift für anorganische Chemie 111 (*1920), pp 78–89.
9. M. Kuehn: *Untersuchung der Verzunderung von unlegiertem Stahl in Gasatmosphären aus Sauerstoff, Kohlendioxid und Stickstoff mit geringen Sauerstoffkonzentrationen*, TU Berlin, 1974.
10. D. Filatov: *Zunder beim Warmwalzen von Stahl: Bildung, Verhalten im Walzspalt und Beizbarkeit*, Max-Planck-Institut für Eisenforschung, 2006.
11. R.I. Olivares et al.: Thermogravimetric Study of Oxidation-Resistant Alloys for High-Temperature Solar Receivers. *Jom* 65 (2013) 12, pp 1660–1669.
12. W. Rasp and D. Filatov: *Zunderbildung beim Warmwalzen*, Max-Planck Hot Forming Conference Dec. 5th 2002.
13. D. Monceau and B. Pieraggi, *Oxidation of Metals* 50 (1998) 5/6, pp 477–493.
14. Sobotka, C., H. Antrekowitsch and H. Schnideritsch: *Burnt to a crisp? – Why oxygen enhanced combustion doesn't have to influence steel oxidation*, Shechtman International Conference, 2014, in press.
15. Deutsche Edelstahlwerke: *Rost-, säure- und hitzebeständige Stähle*, 2010.
16. Böhler Edelstahl GmbH und Co KG: *Böhler H525*, 2002.
17. V. Deodeshmukh and S. Srivastava: The Oxidation performance of modern high-temperature alloys. *Jom 61* (2009),pp 56–59.
18. D. Klarstrom and S. Srivastava: Selection of High Performance Alloys for High Temperature Corrosion Environments. *Corrosion Science (*2005)